Asian Journal of Chemistry; Vol. 37, No. 9 (2025), 2265-2273
ASIAN JOURNAL OF CHEMISTRY
https://doi.org/10.14233/ajchem.2025.34233

Synthesis and Structure of Novel Ruthenium(II) Mixed Ligands Complexes: Density Functional Theory, DNA Binding and Antimicrobial Studies *via* PACT Therapy

T. MANJURAJ[1], P.N. PRASHANTH KUMAR[1,*], B.C. VASANTHA KUMAR[1], MOHAMMED IMADADULLA[1], H.P. SHIVARUDRAPPA[2], SALEEM M. DESAI[3] and M.R. LOKESH[4]

[1]Department of Chemistry, D.R.M. Science College, Davangere-577004, India
[2]Department of Chemistry, G.M. University, Davangere-577006, India
[3]Department of Chemistry, Anjuman Art's, Science & Commerce College, Vijayapur-586101, India
[4]Department of Chemistry, H.K.B.K. College of Engineering, Bangalore-560045, India

*Corresponding author: E-mail: p.n.prashanthkumar@gmail.com

Received: 12 June 2025 *Accepted*: 18 August 2025 *Published online*: 30 August 2025 AJC-22108

Ruthenium(II)-based complexes exhibited efficient light-harvesting capabilities that facilitate the enhanced generation of hydroxyl radicals, thereby significantly promoting antibacterial activity. The novel Ru(II) complexes can be represented as $[Ru(II)(bfq)(bipy)]Cl_2$ (**Ru-L1**), $[Ru(II)(bpdc)(bipy)_2]Cl_2$ (**Ru-L2**) and $[Ru(II)(bfq)(NCS)_2]Cl_2$ (**Ru-L3**), where bfq = benzofuranquinoline carboxylic acid and bipy = bipyridine. The synthesized Ru(II) complexes were characterized with ^1H NMR, IR and UV-visible techniques. The physical measurements such as viscosity measurements and denaturation thermal studies explore the behaviour of DNA binding of the synthesized Ru(II) complexes. In this context, the studies on DFT, molecular electrostatic potential and antimicrobial photodynamic therapy against *Escherichia coli* cells were also conducted. The obtained results show significant inhibition growth of bacterial cells was determined *via* PACT therapy.

Keywords: Ru(II) complexes, DNA binding studies, Viscosity measurements, Denaturation thermal studies, DFT, PACT studies.

INTRODUCTION

In recent decades, biological chemistry has considerably benefited from the utilization of mixed ligand complexes as seen by the numerous natural and synthesized ligands that contain nitrogen and oxygen as donor atoms [1]. Such complexes led to a trend of research for interact with DNA in order to find uses in biotechnology and medicine. Despite their widespread use, carboplatin and cisplatin have a number of adverse effects [2,3]. Consequently, the preparation of chemotherapeutic medications with little or no adverse effects is our primary goal. As a result of the interaction between drugs and DNA, which causes DNA damage in cancer cells and subsequently prevents the cancer cells from dividing and ultimately results in cell death, numerous biological studies have shown that DNA is the primary intracellular target of anticancer drugs [4-6].

In biological chemistry, the use of mixed ligand complexes holds tremendous significance as it enables the development of enhanced selectivity and sensitivity. Studies on 1,10-phenanthroline (phen 1) mixed-ligand chelate systems could provide insight into the mechanisms controlling the synthesis of these mixed ligand complexes [7]. It is particularly important to examine complexes that contain ligands with nitrogenated aromatic rings, as they have shown the ability to break DNA strands [8]. Indeed, it has been demonstrated that a number of metal complexes of sulfur–nitrogen chela-ting compounds exhibit verified cytotoxic properties. In additionally, in an effort to find less toxic and more targeted anticancer treatments, Fe(II) complexes with ligands that contain sulphur and nitrogen are the focus of extensive biological studies [9].

An alternative antibacterial, antifungal and antiviral treatment for drug-resistant organisms is photodynamic antimicrobial chemotherapy (PACT), a recently developed therapeutic option that uses photosensitive molecules and visible light to cause oxidative damage to microbial pathogen [10]. Photodynamic treatment (PDT) for cancer uses compounds that can

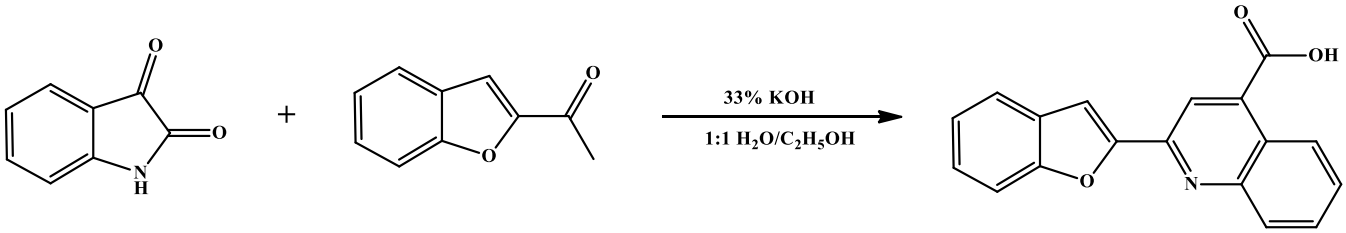

Scheme-I: Synthesis of 2-[N-hydroxy ethanimidoyl] quinoline-4-carboxylic acid] (bfq)

cleave DNA when exposed to light [11]. To minimize toxicity to the surrounding healthy cells, photoactive pro-drugs with limited discharge of a cytotoxic agent exclusively at the irradiation spot can boost selectivity. Oxygen radical species can be obtained through the Fenton reaction, which is an important route when transition metal ions are present. Different types of damage are induced in DNA by these reactive oxygen species. Fe^{2+} ions are one type of these transition metal ions that cleaves DNA. Given that iron is a necessary component of nature for Fenton reaction, leads to the cleavage of both normal and abnormal biological components, including lipids, DNA and proteins [12]. As a result, scientists are currently creating photosensitive metal complexes to deliver cytotoxic medications to precise locations while lessening the toxicity of other healthy cells. To increase the selectivity of cytotoxic activity, the mixed complexes containing a nitrogen ring which are worthier supporting the cleavage of DNA strands. One type of less toxic and more potent anticancer medication is the Ru(II) complex, which contains nitrogen donor ligands. Therefore, we present the synthesis, DNA binding and the antimicrobial PDT of Ru(II) mixed ligand complexes **1-3**, where bipyridine acts as a photosensitizer and benzofuranquinoline carboxylic acid acts as DNA binders.

EXPERIMENTAL

The required chemicals and solvents were of AR grade. Agarose and ethidium bromide were purchased from Himedia (India). Ruthenium(II) chloride, 1,10-phenenthroline and tris HCl were purchased from Merck Ltd. (India). Calf thymus (ct) DNA was procured from Genie, Bangalore (India). tris-HCl buffer solution was dissolved in double distilled deionized water and used to DNA binding studies. Shimadzu 1650 spectrophotometer was used to measure the electronic spectra of the synthesized mixed-ligand Ru(II) complexes. Viscosity measurements were carried out on the semi-micro dilution of viscometer at room temperature. The functional groups were analyzed by infrared spectra using KBr pellets on Shimadzu (Kyoto, Japan) FTIR-8400 instrument. ^{1}H NMR spectra were recorded by Bruker FT-NMR spectrometer. For photocatalytic activity of *E. coli* cells were carried out under monochromatic light of power source *i.e.* 500 W halogen – tungsten lamp was used.

Synthesis of 2-[*N*-hydroxyethanimidoyl]quinoline-4-carboxylic acid] (bfq): The formulated product of 2-(1-benzofuran-2-yl)quinoline-4-carboxylic acid was synthesized by Pifitzinger method [13]. Briefly, in the presence of alkaline conditions (33% KOH in water), 2-acetyl benzofuran and isatin solution was refluxed for about 4 h with constant stirring, correspondingly TLC was also monitored for conforming the formation of desired product. The yellow precipitate was obtained by neutralizing with 10% of dilute HCl (**Scheme-I**). Yield: 72%. m.p.: 244-247 ºC (lit. 248-250 ºC [13]). ^{1}H NMR (400 MHz, DMSO-d_6, δ ppm): 8.5 (s, 1H quinoline 3C–H), 8.20 (d, 1H, ArH), 7.89 (t,1 H, ArH),7.8 (q, 2H, ArH), 7.93 (d, 1H, ArH), 7.72 (t, 1H, ArH), 7.32 (t, 1H, ArH), 8.7 (d, 1H, ArH), 7.36 (t, 1H, ArH) and 14.10 (s, 1H, COOH).

Synthesis of 3,3′-dicarboxy-2,2′-bipyridine [bpdc]: Another key product 3,3′-dicarboxy-2,2′-bipyridine was synthesized according to the reported method [14]. The melting point was 260 ºC (decomposition), which is consistent with the reported value of 258 ºC (**Scheme-II**).

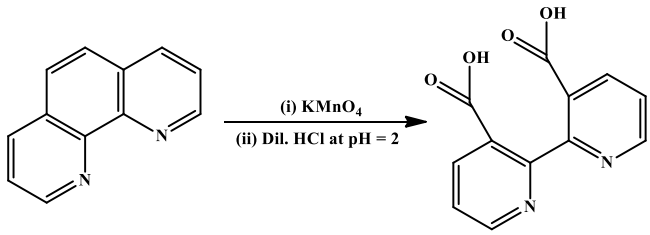

Scheme-II: Synthesis of 3,3′-dicarboxy-2,2′-bipyridine [bpdc]

Synthesis of *cis*-dichloro(2,2′-bipyridyl)(benzofuran-quinoline-carboxylic acid) ruthenium(II) complex [(Ru(II)-(bipy)(bfq)Cl$_2$] (Ru-L1): In a 50 mL of two-necked flask, $RuCl_3 \cdot 3H_2O$ (0.075 g, 0.282 mmol) in 30 mL of DMF was added to bipyridyl (0.045 g, 0.282 mmol) in ethanol with constant stirring and heated to ~90 ºC in dark for 2 h under nitrogen atmosphere. Then, added 0.085 g (0.282 mmol) of 2-[N-hydroxy ethanimidoyl]quinoline-4-carboxylic acid] (L1) to the resulting solution and heated to 120 ºC with constant stirring for an additional 5 h. Finally, a red coloured solid product was obtained and then purified by chromatography with dichloromethane/methanol (9/1) as eluent to afford the corresponding complex (55% yield). ^{1}H NMR (400 MHz, DMSO-d_6, δ ppm): 14.102 (s, 1H, COOH), 8.83-8.81 (d, 1H Ar–H), 8.7-8.684 (d, 1H), 8.48 (s, 1H, Ar–H), 8.17-8.14 (d, 2H, Ar–H), 7.9 (d,1H, Ar-H), 7.89 (t,1H, Ar–H), 7.79-7.76 (q, 3H, Ar–H), 7.72-7.7 (t, 3H, Ar–H), 7.53-7.5 (t,1H, Ar–H). 7.46-7.42 (t, 2H, Ar–H), 7.36-7.32 (t, 2H, Ar–H.

Synthesis of [*cis*-dithiocyanato (benzofuran quinoline carboxylic acid)ruthenium(II) chloride] [Ru(bfq)(NCS)$_2$Cl$_2$] (Ru-L3): The Ru-L3 complex was synthesized by refluxing [Ru(bipy)(bfq)(Cl)$_2$] (~ 280 mg) in dark by dissolving it in 30 mL of methanol. Added 20 mL 0.1 M NaOH aqueous solution to this solution to deprotonate the carboxyl group.

The sodium thiocyanate solution (350 mg, 2 mL of water was added to the above mixture and refluxed for 24 h. The resulting filtrate solution was monitored at pH was adjusted to 2 by using dilute $HClO_4$. The red coloured solution completely changed into yellow colour due to the replacement of bipyridyl to chloride ligand, which was confirmed by IR studies. The possible reason for substitution of these moieties may be due to the steric hindrance of the complex. The buff-coloured precipitate was washed thoroughly with distilled water followed by anhydrous diethyl ether and air-dried for 1 h. Yield: 74%. ^{1}H NMR (400 MHz, DMSO-d_6, δ ppm): 14.1 (s, 1H,COOH), 8.7 (d, 1H, Ar–H), 8.53 (s, 1H, Ar–H), 8.24 (d, 1H), 7.96 (d, 1H, Ar–H), 7.9 (t, 1 H, Ar-H), 7.84 (q, 2H,Ar–H), 7.73 (t, 1H, Ar–H), 7.46 (t, 1H, Ar–H), 7.35 (t, 1H, Ar–H).

Synthesis of [*bis*(2,2′-bipyridyl) (3,3′-dicarboxy-2,2′-bipyridine) ruthenium(II)] complex [Ru(bipy)$_2$(3,3′-dcbipy)] [Ru-L2]: 3,3′-Binicotinic acid (0.21 mmol, 50 mg) in 25 mL of ethanol was reacted with $(bipy)_2RuCl_3 \cdot 2H_2O$ (0.2 mmol, 100 mg), which served as a precursor for the synthesis of Ru-L2 following the reported procedure [15].

The structure of the synthesized mixed ligands Ru(II) complex are shown in Fig. 1.

DNA binding experiments: DNA binding experiments were carried out according to the described experimental procedure [16]. The required concentration of the *ct*-DNA and complex solutions were prepared by serial dilution method. The absorption studies were carried out by adding the increasing concentrations (0-25 µM) of *ct*-DNA to 50 µM of complex solutions. A plot of $[DNA]/(\varepsilon_a-\varepsilon_f)$ *versus* [DNA] was drawn, the intrinsic binding constant (K_b) was measured from the following equation:

$$\frac{[DNA]}{(\varepsilon_a-\varepsilon_f)}=\frac{[DNA]}{(\varepsilon_b-\varepsilon_f)}+\frac{1}{K_b(\varepsilon_b-\varepsilon_f)}$$

The delivered variables such as ε_a, ε_f and ε_b are the extinction coefficients of apparent, free and bound metal complex. Based on the experimental values, a graph was drawn between the ratio of $[DNA]/(\varepsilon_b-\varepsilon_f)$ against [DNA]. To determine the slope, $1/(\varepsilon_b-\varepsilon_f)$ can be obtained by drawing a line graph and the intercept is equal to $1/K_b(\varepsilon_b-\varepsilon_f)$, where K_b is the ratio of slope to the intercept.

Viscosity measurement: The relative viscosity (η) was calculated according to the relation $\eta = (t-t_0)/t$, where t is the flow time of DNA in the presence or absence of complex and t_0 is the flow time of buffer alone. The mode of binding between *ct*-DNA and metal complexes can be understood by the viscosity measurements. The viscosity measurement was carried out by adding varying amounts of complex solutions (50 to 200 µM) to *ct*-DNA (100 µM of *ct*-DNA in tris HCl/NaCl buffer) at 37 ± 0.1 ºC. Flow times were measured in triplicate using a digital stopwatch and the average was recorded. Viscosity measurements were evaluated by plotting $(\eta/\eta_o)^{1/3}$ *vs.* the binding ratio, where η is the viscosity of DNA in the presence of complex, and η_0 is the viscosity of DNA alone in acidic buffer medium [17].

Thermal denaturation: This technique significantly influenced the experiment by measuring the absorption behaviour of *ct*-DNA and all three Ru(II) complexes under a temperature variation of approximately 5–10 ºC. Notably, the absorption maxima of all complexes remained constant at high wavelengths. The melting temperature (T_m) of the DNA–complex adducts increased compared to that of free *ct*-DNA (50 µM). This increase suggests stronger stabilization of the DNA duplex by the complexes, as the thermal denaturation process reflects the transition of double-stranded DNA to single-stranded DNA with rising temperature [18].

Computational studies: The Gaussian 09W program was used to conduct all the computational calculations for the synthesized mixed-ligand Ru(II) complexes. The molecular geometries of the singlet ground states of the complexes were fully optimized in the gas phase using DFT with the B3LYP functional. Two different basis sets were employed using 6-31G(d,p) and LANL2DZ. The HOMO (highest occupied molecular orbital) and LUMO (lowest unoccupied molecular orbital) border molecular orbitals of the investigated compounds were depicted using the auxiliary application chemcraft with chem 3D and Gaussian view [19].

PACT assay: The antimicrobial activities were evaluated following procedures as reported in the literature [20,21]. *E. coli* ATCC-25922 were an anaerobically grown using Luria-Bertani (LB) broth (1% tryptone, 0.5% yeast extract, 0.5% NaCl w/v) at 37 ºC. The novel Ru(II) complexes was dissolved

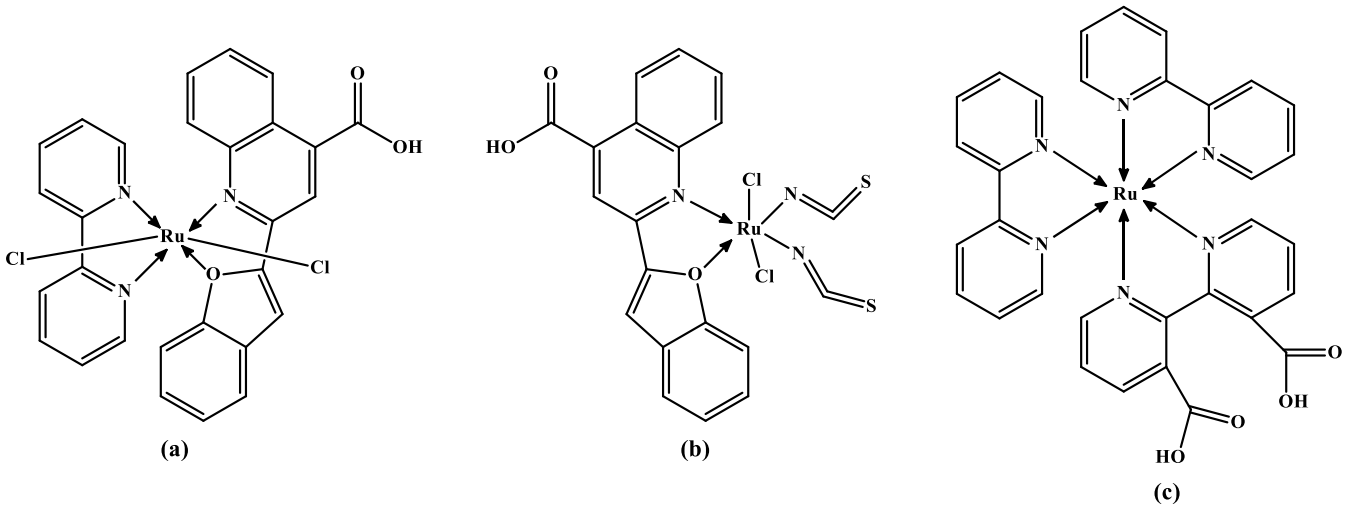

Fig. 1. Structures of (a) Ru-L1, (b) Ru-L3, (c) Ru-L2 complexes

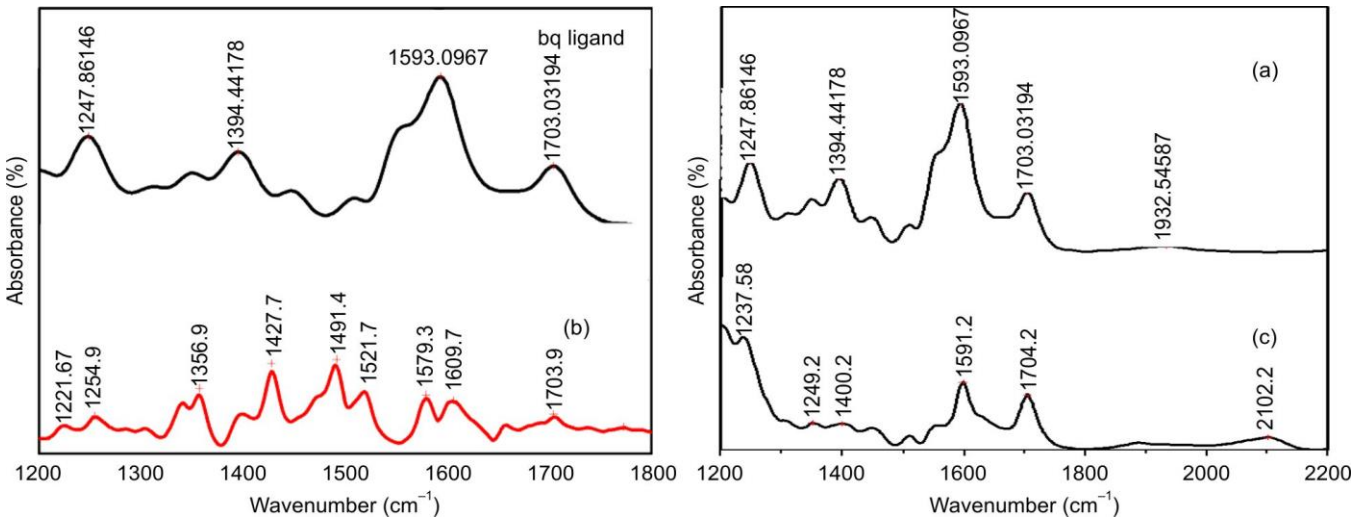

Fig. 2. IR spectra of (a) bfq molecule, (b) [Ru(II)(bfq)(bipy)(Cl_2)] and (c) [Ru(II)(bq)($NCS)_2$(Cl_2)]

in DMSO solvent and it was maintained the concentrations of about 25 and 50 µM were used for investigation for this analysis. The bacterial cultures were grown on LB Broth, it was diluted with 20 mL of buffer solution which notes that the visibility of cell density was counted to be 10^8 cfu mL^{-1}. The filled solution was incubated in a foil-covered tubes due to protect the exposure of light.

Meanwhile, the diluted solutions were exposed to 500 W halogen–tungsten lamp positioned approximately 20 cm above the samples, with continuous magnetic stirring maintained throughout the exposure. The control cultures were monitored with the absence and presence of complexes with exposed to particular wavelength. Later, the aliquots were diluted and it was cultured in LB agar medium. Before and after exposure of irradiation of particular wavelength with samples was used to calculate the survival percentage ($N_1/N_0 \times 100$) of *E. coli* cells, where, N_o and N_1 are before and after counting the cell colonies based on cfu mL^{-1}.

RESULTS AND DISCUSSION

ATR-IR spectral studies: The Ru(II) complexes were placed in an attenuated total reflectance (ATR) accessory equipped with a single reflection ZnSe element. The vibrational spectral bands of all complexes were recorded in the range of 4000-400 cm^{-1}. The most prominent vibrational bands were analyzed in the range 1800-1000 cm^{-1}. For C-O stretching bands indicates that the symmetric and asymmetric vibrations are present in these complexes. The obtained IR spectra of benzofuran quinoline carboxylic acid exhibits the vibrational bands which was followed as C=O stretching band at 1703 cm^{-1}, C=N at 1593 cm^{-1}; (-C-O-C) asymmetric stretch at 1247 cm^{-1} and a band at 1394 cm^{-1} is because of (CO^{2-}) stretching is as shown in Fig. 2a.

The major IR bands of Ru-L1 molecule are as follows: 1703.9 cm^{-1} (C=O) stretching mode; broad band at 1609.7 cm^{-1} (overlapping the highest bipy band), which was assigned to 1356.9 cm^{-1} for the symmetric stretching of CO^{2-}; 1254.9 cm^{-1} for singly bonded C-O stretching. The peaks at 1609.7, 1521.7, 1491.4 and 1427.7 cm^{-1} shows the appearance of bipyridyl bands and 1579.3 for C=N stretching of benzofuran quinoline ring (over lapping C=N of bipyridyl). The above fact describes that both C=O and CO_2 stretching bands were freely flagged, which indicates both protonated and deprotonated carboxylic groups are present in the Ru-L1 complex.

The primary IR bands of Ru-L3 were as follows: 1151.8 cm^{-1} for C-O-H bending; 1237.8 cm^{-1} for singly bonded CO stretching; 1704.2 cm^{-1} for C=O stretching mode. Instead, a broad band was observed at 1618.1 cm^{-1}, which was assigned to the anti-symmetric stretch of CO_2, where the negative charge is delocalized to produce two equivalent (or nearly equivalent) C-O bonds and a peak at 2102 cm^{-1}, which is assigned to the NCS-bonded Ru(II) metal ion is as shown in Fig. 2c [22,23].

Similarly, the main infrared bands of the Ru-L2 complex are as follows: The C=O stretch mode obtained as 1728 cm^{-1}; there is a strong broad band at 1598.4 cm^{-1} (overlapping the highest bipy band) designated as symmetric anti-stretch CO_2 of bpdc ligand, where the negative charge is delocalized to produce two equivalent CO bonds (or almost such); 1341 cm^{-1} for CO_2 symmetric stretching; 1273 cm^{-1} for single bond CO stretching; the bipy vibration peak was 1598, 1540, 1463 and 1428 cm^{-1}. The as shown values agree with the literature on the bipy ring stretch of [Ru(bipy)$_3$] complex as shown in Fig. 3.

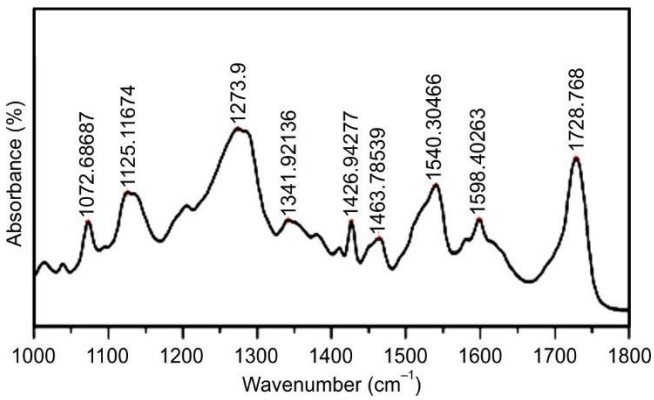

Fig. 3. IR spectra of [Ru(II)(bpdc)(bipy)$_2$]Cl_2 complex

Optical properties of complexes: Optical spectra of Ru-L1, Ru-L2 and Ru-L3 complexes were recorded in DMF solvent. The absorption spectra of Ru-L2 complex shows an intense UV band at 291 nm, which was assigned to ligand-centered π to π* transitions. A broad band at 453 nm assigned to metal-to-ligand charge-transfer (MLCT) transition (*i.e.* d→π*) as shown in Fig. 4a. Similarly, the spectrum of Ru-L1 complex showed two UV bands between 200-400 nm. Among them an intense band at 290 nm was observed due to ligand-centered π to π* transitions [24].

Another band appeared at 354 nm corresponds to ligand-centered π to π* transitions and a broad band obtained at 455 nm was assigned to metal-to-ligand charge-transfer (MLCT) transitions *i.e.* (d to π*) is as shown in Fig. 4b. The spectral pattern of Ru-L3 complex gave a new peak around 520 nm. The band at 520 nm is well extended to the 600 nm region of the spectrum as shown in Fig. 4c. This effect may be due to the stronger electron donating effect of the thiocyanate ligand causes an increased energetic destabilization of the Ru(t_{2g}) level. Shifting the Ru (t_{2g}) higher energy level which influences the decrease in transition energy from Ru center to NCS ligand, based on the above facts influences shifting the wavelength towards longer wavelength.

DNA binding studies: The UV-visible absorption spectra of Ru(II) complexes in absence and presence of *ct*-DNA was observed. The absorption spectra of all Ru(II) complexes show significant hyperchromism with increasing the concentration of *ct*-DNA from 0 to 25 µM, with a slight redshift of ~ 2-3 nm (Fig. 5a-c). Similar absorption pattern was observed from the relevant literature with similar type of ligands [17,25]. The binding constants (K_b) of Ru(II) complexes such as Ru-L1, Ru-L3 and Ru-L2 were 2.1×10^4, 1.1×10^3 and 3.2×10^4 M^{-1}, respectively. The obtained K_b values for synthesized complexes are lower than that of the classical intercalator, ethidium bromide (EB) whose K_b value was of the order of 10^6–10^7 M^{-1}. Thus, it can be concluded that all the synthesized Ru(II) complexes binds to *ct*-DNA through groove binding as supported by the hyperchromism [26].

However, there is a slight red shift is expected due to stacking of aromatic moiety within the DNA base pairs. Based on the above facts, all the synthesized Ru(II) complexes bind to *ct*-DNA *via* partial intercalation. By comparing the K_b values of the Ru(II) complexes under study, complex Ru-L2 with bipyridyl analogs exhibit a relatively high tendency to bind to DNA.

Viscosity measurements: In current study, the relative viscosity was calculated for all the complexes under study at a ratio (r), where r is [complex]/[DNA] which varies from 0.00 and 0.40 with an interval of 0.1. The DNA concentration remains the same, while the metal complex concentration is varying. The relative viscosity (η/η_o) were plotted against [complex]/[DNA]. From the plot (Fig. 6), it clearly shown that there is a decrease in relative viscosity with increasing value of r, suggesting a non-intercalative mode of binding with *ct*-DNA. The decrease in relative viscosity is due to kink or bend in the *ct*-DNA strand, leading to diminished length [27]. The experimental results suggested that the all the Ru(II) complexes bind to *ct*-DNA in a groove binding.

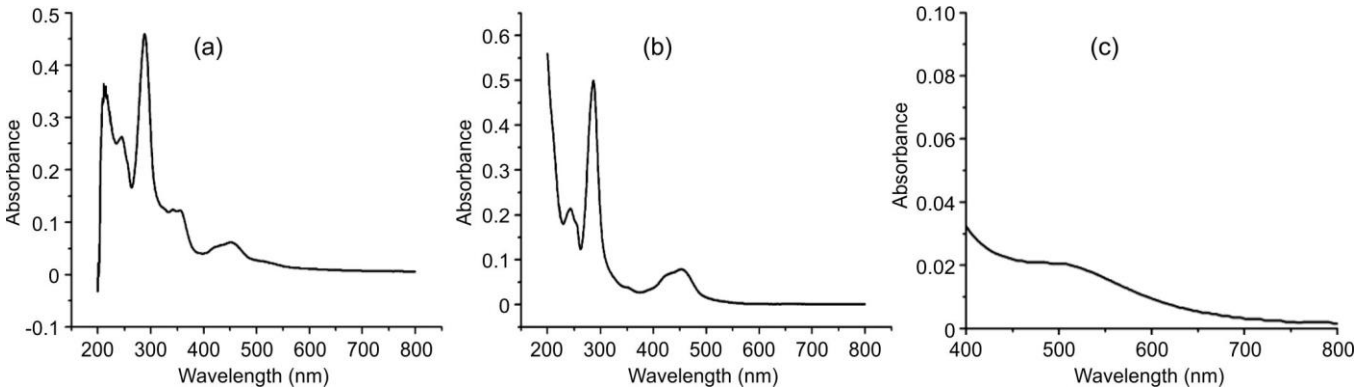

Fig. 4. Absorbance spectra of (a) Ru-L1 (b) Ru-L2 and (c) Ru-L3 complexes

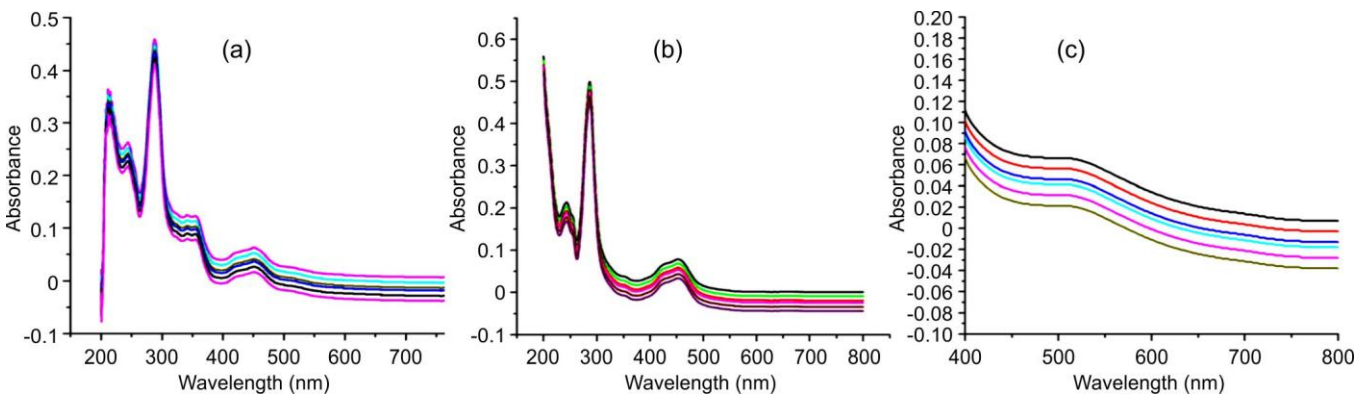

Fig. 5. DNA binding studies of (a) Ru-L1 (b) Ru-L2 and (c) Ru-L3 complexes

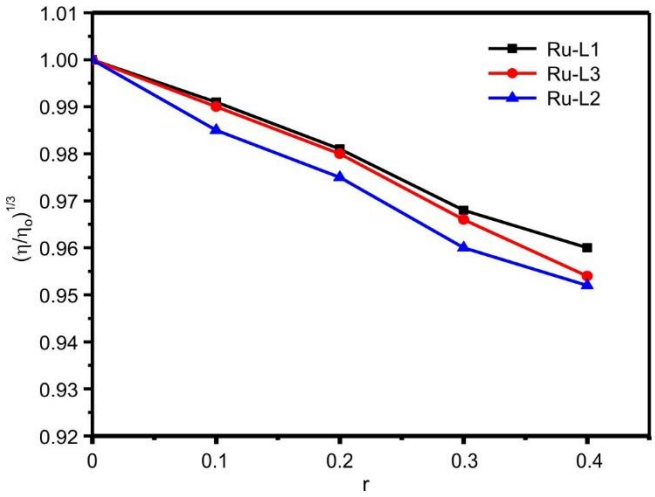

Fig. 6. Viscosity measurements of (a) Ru-L1 (b) Ru-L3 and (c) Ru-L2 complexes

Thermal denaturation: DNA fusion is a process in which double-stranded DNA gradually dissociates into single strands by breaking hydrogen bonds between bases, which produces a colour-enhancing effect in the absorption spectrum of DNA base pairs close to 260 nm. The thermal melting temperature (T_m) is the temperature at which half of the DNA strand is in a double helix state and the other half is in a random spiral state. The increase of the thermal melting temperature of (T_m) indicates interaction between DNA and metal complex [7,28].

In this case, the T_m value was determined by knowing the experimental absorbance of the DNA at 260 nm as a function of temperature. When adding Ru(II) complexes to DNA, a moderate positive shift (ΔT_m) of the melting temperature (ΔT_m) of DNA was observed in the range of 1.4 to 3.8 ºC (Fig. 7). This modest increase in T_m is comparable to observed with other groove binders [29,30]. The thermal denaturation test result is consistent with absorption spectrum curve and viscosity measurement result.

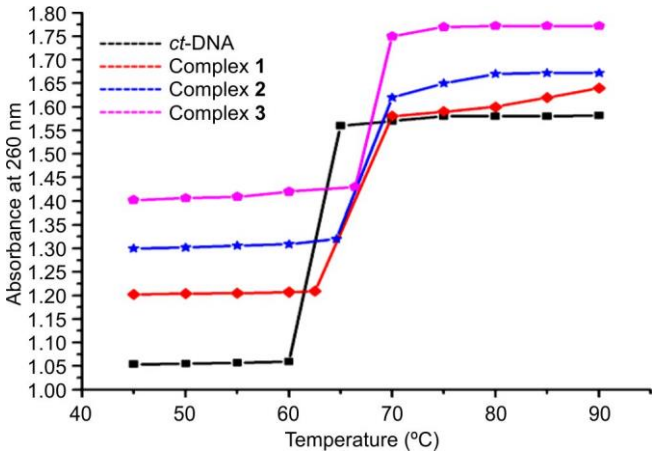

Fig. 7. Thermal denaturation studies of (a) complex-1 (Ru-L1) (b) complex-2 (Ru-L3) and (c) complex-3 (Ru-L2) complexes

Computational studies: The structure of all the Ru(II) complexes was optimized through B3LYP 6-31G(d,p) method and are shown in Figs. 8 and 9. The frontier molecular orbital (FMO) energy gaps provide insight into the kinetic stability and chemical reactivity of the complexes. The FMO energy trends for the Ru(II) complexes suggest that the Ru-L3 complex exhibits a higher reactivity, as indicated by its smaller band gap of 1.331 eV, compared to Ru-L1 and Ru-L2, which have slightly larger band gaps of 2.173 eV and 1.621 eV, respectively. It can be seen that HOMO and LUMO are centered on the moiety and molecular skeleton. A molecule with a small FMO gap is generally associated with a high chemical reactivity and low kinetic stability [31,32].

Molecular electrostatic potential (MEP) illustrates the 3D charge distribution, which correlates the molecular structure and physico-chemical properties of the molecules. The negative electrostatic potential corresponds to a proton attraction by the electron density of the molecules and is indicated in the red region. In regions with low electron density, the positive electrostatic potential corresponds to the repulsion of proton by the atomic nuclei and is indicated in blue and the region of zero potential as green. From Fig. 10, it is observed that the most negative electrostatic potential is attributed as Ru-L1 moiety, the more positive electrostatic potential is found to be Ru-L2 group and Ru-L3 behaves as zero potential [33].

PACT studies: It detects that all the synthesized Ru(II) complexes was tested for its ability to kill *E. coli* by irradiating with a 500 W halogen lamp. The survival existed rate of cells under visible light irradiation of 500 W halogen tungsten lamp to obtain reliable data on the viable efficacy of photodynamic treatment in *E. coli.* Initially, the experiment was evaluated that in the absence of complex, the *E. coli* culture (10^8 cfu mL^{-1}) was irradiated for 60 min and no significant reduction in the number of viable cells was observed. Therefore, in all PACT measurements, the irradiation time was maintained for 60 min.

To standardize the incubation time with complex before incident to light, (10^8 cfu mL^{-1}) bacterial suspension was incubated with complex in the dark for 30, 60 and 90 min, using in phosphate buffer wash once with normal saline and then irradiate with light for a predetermined for 60 min of time. The survival rate of cases of *E. coli* during the presence of light treatment was found to be 0.043, 0.042, 0.044%. The benchmarked results do not influence the contact time and bare incident light for bacterial cells does not improve the performance of the inhibition of *E. coli* bacteria. Further standardized the *E. coli* PDT program was used to test based on concentration of the complexes. The obtained data tells that increasing the concentration of complexes up to 50 µg mL^{-1} the viability of the bacterial cells was reduced slightly [34].

E. coli showed a significant dose-dependent lethality when exposed to different complexes at concentrations of 25 and 50 µM. The viability of *E. coli* colonies was determined by counting colony-forming units (CFU). The effects of the control, individual Ru(II) complexes (Ru-L1, Ru-L2 and Ru-L3) and their light-irradiated forms were assessed at varying concentrations to evaluate the efficacy of photodynamic therapy (PDT). The CFU (%) after treatment reflects the PDT effectiveness, as illustrated in Fig. 11. Statistical analysis of the *E. coli* survival percentages revealed CFU counts of 8.9%, 11.1%, and 7.8% for the Ru-L1, Ru-L2 and Ru-L3 complexes, respectively compared to the control. It means that

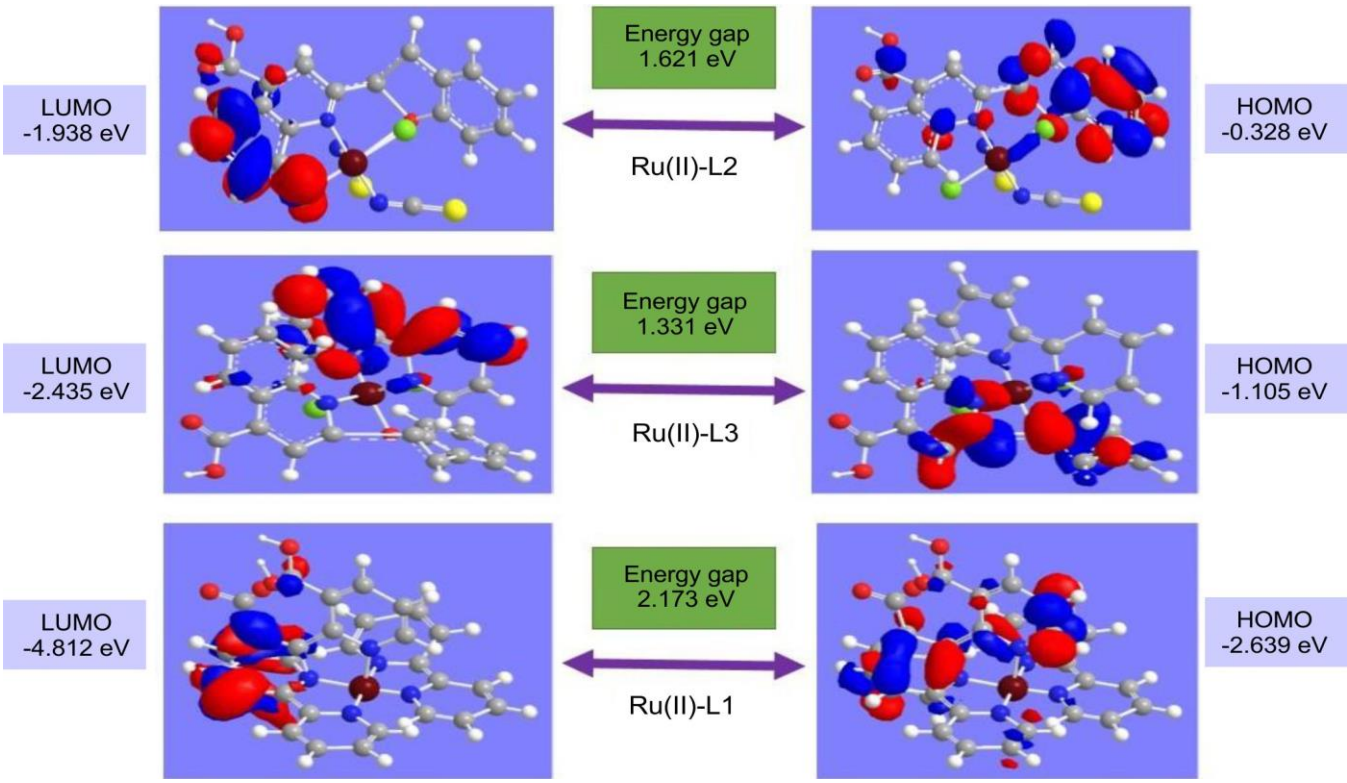

Fig. 8. HOMO-LUMO energy gap of Ru(II) complexes

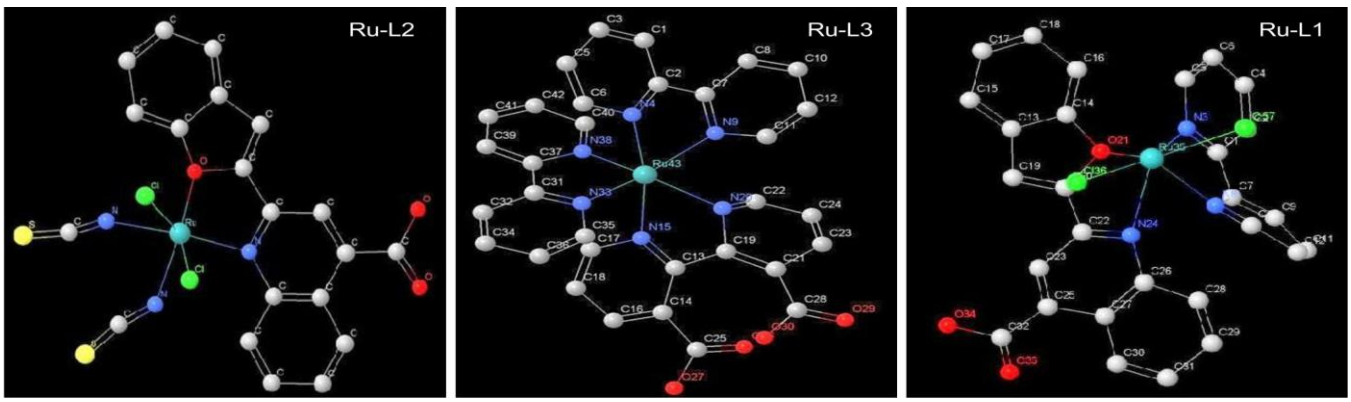

Fig. 9. Optimized geometry of Ru(II) complexes

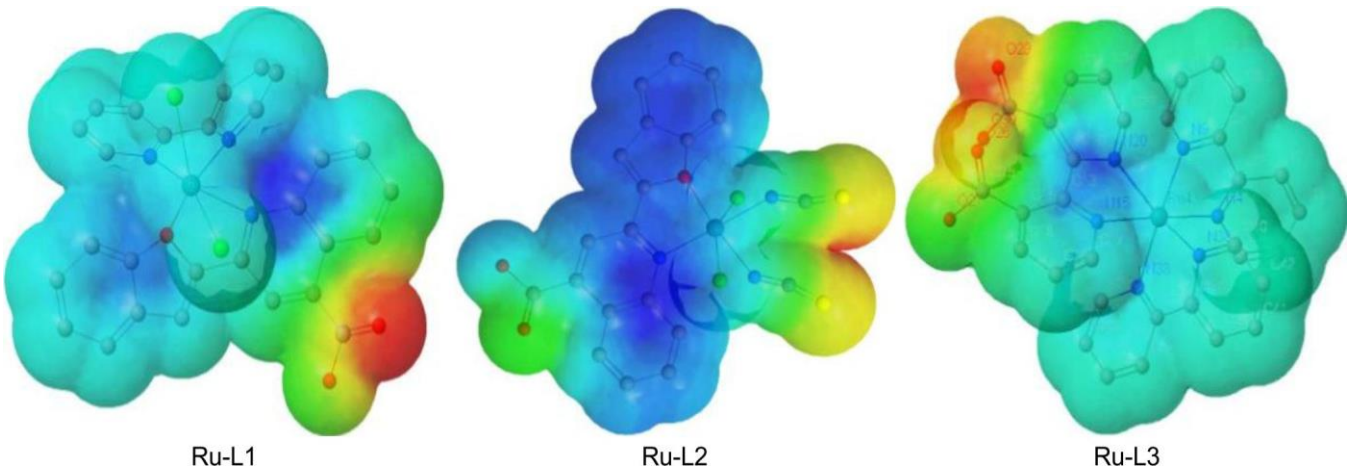

Fig. 10. MEP surfaces of Ru(II) complexes

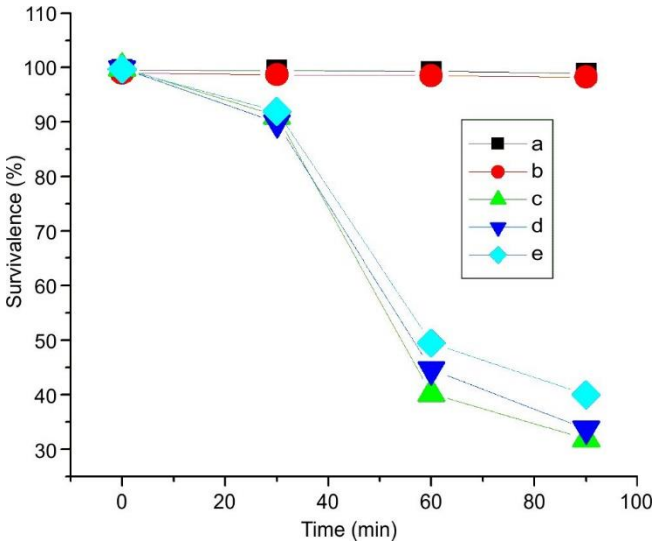

Fig. 11. PACT studies of (a) control (b) dark condition with presence of complexes (c) Ru-L2 (d) Ru-L1 and (e) Ru-L3 complexes with irradiation of visible light

there is no significant reduction for the viability of the cells using bare complexes. However, significant reductions in the CFU counts were observed at 60.8, 56.2, 51.5% of 25 µM and 69.1, 67.2, 60.4 for 50 µM for inducing light-irradiated complexes of Ru-L2, Ru-L1 and Ru-L3 with respect to the control group.

Conclusion

Two new mixed ruthenium(II) complexes encapsulated by N,O donor of benzofuranquinoline (bfq), N,N-donor bipyridyl base (bipy) and anti-ligand NCS have been synthesized and structurally characterized. The spectra of all Ru(II) complexes shows the visible region which meets the PDT application. DNA binding through non-intercalative mode and groove binding corresponds for inhibiting the growth of bacterial cells. The profound results may indicate that new Ru(II)-based complexes with nitrogen and oxygen-containing ligands can be used in PDT applications and as alternatives to PDT anticancer drugs. Complex RuL2 performs greater binding and hyper chromic spectrum compared with other complexes, hence it behaves as greater potential than other complexes for PDT therapy.

ACKNOWLEDGEMENTS

The authors are grateful for the facilities provided by the Department of Chemistry of DRM Science College, Davangere and NMKRV College, Bengaluru, India.

CONFLICT OF INTEREST

The authors declare that there is no conflict of interests regarding the publication of this article.

REFERENCES

1. H.R.P. Naik, H.S. Bhojya Naik, T.R. Ravikumar Naik, H.R. Naika, K. Gouthamchandra, R. Mahmood and B.M.K. Ahamed, *Eur. J. Med. Chem.*, **44**, 981 (2009); https://doi.org/10.1016/j.ejmech.2008.07.006
2. V.F. Vasconcellos, G.N. Marta, E.M.K. da Silva, A.F.T. Gois, T.B. de Castria and R. Riera, *Cochrane Database Systemat. Rev.*, **2020**, CD009256 (2020); https://doi.org/10.1002/14651858.CD009256.pub3
3. R. Oun, Y.E. Moussa and N.J. Wheate, *Dalton Trans.*, **47**, 6645 (2018); https://doi.org/10.1039/C8DT00838H
4. T.G.A. Reuvers, R. Kanaar and J. Nonnekens, *Cancers*, **12**, 2098 (2020); https://doi.org/10.3390/cancers12082098
5. M. Sharma, P. Anand, Y.S. Padwad, V. Dogra and V. Acharya, *Free Radic. Biol. Med.*, **178**, 174 (2022); https://doi.org/10.1016/j.freeradbiomed.2021.11.033
6. S.U. Khan, K. Fatima, S. Aisha and F. Malik, *Cell Commun. Signal.*, **22**, 109 (2024); https://doi.org/10.1186/s12964-023-01302-1
7. M.C. Prabhakara, H.S. Bhojya Naik, H.M. Kumaraswamy and V. Krishna, *Nucleosides Nucleotides Nucleic Acids*, **26**, 459 (2007); https://doi.org/10.1080/15257770701426237
8. B. Sreekanth, G. Krishnamurthy, H.S. Bhojya Naik and T.K. Vishnuvardhan, *Nucleosides Nucleotides Nucleic Acids*, **31**, 1 (2012); https://doi.org/10.1080/15257770.2011.636415
9. N. Sunitha, C.I.S. Raj and B.S. Kumari, *Res. Chem.*, **4**, 100588 (2022); https://doi.org/10.1016/j.rechem.2022.1005881196
10. S.A. Rupa, M.A.M. Patwary, W.E. Ghann, A. Abdullahi, A.K.M.R. Uddin, M.M. Mahmud, M.A. Haque, J. Uddin and M. Kazi, *RSC Adv.*, **13**, 23819 (2023); https://doi.org/10.1039/D3RA04364A
11. J. Joseph and B.H. Mehta, *Russ. J. Coord. Chem.*, **33**, 124 (2007); https://doi.org/10.1134/S1070328407020091
12. N. Agrawal, R. Mishra, S. Pathak, A. Goyal and K. Shah, *Lett. Org. Chem.*, **20**, 123 (2023); https://doi.org/10.2174/1570178619666220831122614
13. M. Chen, X. Chen, G. Huang, Y. Jiang, Y. Gou and J. Deng, *J. Mol. Struct.*, **1268**, 133730 (2022); https://doi.org/10.1016/j.molstruc.2022.133730
14. K. Abe, K. Matsufuji, M. Ohba and H. Okawa, *Inorg. Chem.*, **41**, 4461 (2002); https://doi.org/10.1021/ic020002f
15. H.Q. Chang, L. Jia, J. Xu, W.N. Wu, T.-F. Zhu, R.-H. Chen, T.-L. Ma, Y. Wang and Z.-Q. Xu, *Transition Met. Chem.*, **40**, 485 (2015); https://doi.org/10.1007/s11243-015-9938-x
16. X.-Q. Zhou, Y. Li, D.-Y. Zhang, Y. Nie, Z.-J. Li, W. Gu, X. Liu, J.-L. Tian, and S.-P. Yan, *Eur. J. Med. Chem.*, **114**, 244 (2016); https://doi.org/10.1016/j.ejmech.2016.02.055
17. I. Warad, H. Suboh, N. Al-Zaqri, A. Alsalme, F.A. Alharthi, M.M. Aljohani and A. Zarrouk, *RSC Adv.*, **10**, 21806 (2020); https://doi.org/10.1039/D0RA04323K
18. J. Devi, B. Kumar and B. Taxak, *Inorg. Chem. Commun.*, **139**, 109208 (2022); https://doi.org/10.1016/j.inoche.2022.109208
19. B. Kumar, J. Devi, P. Saini, D. Khurana, K. Singh and Y. Singh, *Res. Chem. Intermed.*, **50**, 3915 (2024); https://doi.org/10.1007/s11164-024-05328-z
20. T. Manjuraj, G. Krishnamurthy, Y.D. Bodke and H.S. Bhojya Naik, *J. Mol. Struct.*, **1148**, 231 (2017); https://doi.org/10.1016/j.molstruc.2017.07.020
21. L. Balapoor, R. Bikas and M. Dargahi, *Inorg. Chim. Acta*, **510**, 119734 (2020); https://doi.org/10.1016/j.ica.2020.119734
22. A.B.P. Lever, Inorganic Electronic Spectroscopy, Elsevier, Amsterdam, edn 2, pp. 487 (1984).
23. K. Nakamoto, eds.: J.M. Chalmers and P.R. Griffiths, Infrared and Raman Spectra of Inorganic and Coordination Compounds, In: Handbook of Vibrational Spectroscopy, Chichester, UK: John Wiley & Sons, Ltd. (2006).
24. M. Shebl, M.A. El-Ghamry, S.M.E. Khalil and M.A.A. Kishk, *Spectrochim. Acta A Mol. Biomol. Spectrosc.*, **126**, 232 (2014); https://doi.org/10.1016/j.saa.2014.02.014
25. F.A. Cotton and G. Wilkinson, Advanced Inorganic Chemistry, Wiley Eastern Pvt. Ltd., New Delhi, edn 3 (1972).

26. K.N. Aneesrahman, K. Ramaiah, G. Rohini, G.P. Stefy, N.S.P. Bhuvanesh and A. Sreekanth, *Inorg. Chim. Acta*, **492**, 131 (2019); https://doi.org/10.1016/j.ica.2019.04.019
27. T. Manjuraj, G. Krishnamurthy, Y.D. Bodke, H.S. Bhojya Naik and H.S. Anil Kumar, *J. Mol. Struct.*, **1171**, 481 (2018); https://doi.org/10.1016/j.molstruc.2018.06.055
28. K.R. Sangeetha Gowda, H.S. Bhojya Naik, H.V. Sudeep, B. Vinay Kumar, C.N. Sudhamani, T.R. Ravikumar Naik and G. Krishnamurthy, *Spectrochim. Acta A Mol. Biomol. Spectrosc.*, **105**, 229 (2013); https://doi.org/10.1016/j.saa.2012.12.011
29. R. Arulraj, *J. Mol. Struct.*, **1248**, 131483 (2022); https://doi.org/10.1016/j.molstruc.2021.131483
30. K. Funatsu, T. Miyao and M. Arakawa, *Curr. Computeraided Drug Des.*, **7**, 1 (2011); https://doi.org/10.2174/157340911793743556
31. S. Aslam, M. Haroon, T. Akhtar, M. Arshad, M. Khalid, Z. Shafiq, M. Imran and A. Ullah, *ACS Omega*, **7**, 31036 (2022); https://doi.org/10.1021/acsomega.2c02805
32. K. Upendranath, T. Venkatesh, Y. Arthoba Nayaka, M. Shashank and G. Nagaraju, *Inorg. Chem. Commun.*, **139**, 109354 (2022); https://doi.org/10.1016/j.inoche.2022.109354
33. G. Singh, A. Singh, R.K. Verma, R. Mall and U. Azeem, *Comput. Biol. Chem.*, **72**, 45 (2018); https://doi.org/10.1016/j.compbiolchem.2017.12.010
34. M. Musthafa, R. Konakanchi, R. Ganguly and A. Sreekanth, *Phosphorus Sulfur Silicon Relat. Elem.*, **195**, 331 (2020); https://doi.org/10.1080/10426507.2019.1699924